AIMS Mathematics, 8(9): 21106–21122.
DOI: 10.3934/math.20231075
Received: 15 March 2023
Revised: 25 May 2023
Accepted: 29 May 2023
Published: 03 July 2023

http://www.aimspress.com/journal/Math

Research article

A scale conjugate neural network learning process for the nonlinear malaria disease model

Manal Alqhtani[1], J.F. Gómez-Aguilar[2,*], Khaled M. Saad[1], Zulqurnain Sabir[3,4] and Eduardo Pérez-Careta[5]

[1] Department of Mathematics, College of Sciences and Arts, Najran University, Najran, Kingdom of Saudi Arabia
[2] CONACyT–Tecnológico Nacional de México/CENIDET. Interior Internado Palmira S/N, Col. Palmira, Cuernavaca Morelos C.P. 62490, México
[3] Department of Mathematics and Statistics, Hazara University, Mansehra, Pakistan
[4] Department of Computer Science and Mathematics, Lebanese American University, Beirut, Lebanon
[5] Universidad de Guanajuato, Dpto. Electrónica, Carretera Salamanca-Valle de Santiago, Km 3+1.8, Salamanca Gto, México

Correspondence: Email: jose.ga@cenidet.tecnm.mx; Tel: +527773627770, Ext. 2211.

Abstract: The purpose of this work is to provide a stochastic framework based on the scale conjugate gradient neural networks (SCJGNNs) for solving the malaria disease model of pesticides and medication (MDMPM). The host and vector populations are divided in the mathematical form of the malaria through the pesticides and medication. The stochastic SCJGNNs procedure has been presented through the supervised neural networks based on the statics of validation (12%), testing (10%), and training (78%) for solving the MDMPM. The optimization is performed through the SCJGNN along with the log-sigmoid transfer function in the hidden layers along with fifteen numbers of neurons to solve the MDMPM. The accurateness and precision of the proposed SCJGNNs is observed through the comparison of obtained and source (Runge-Kutta) results, while the small calculated absolute error indicate the exactitude of designed framework based on the SCJGNNs. The reliability and consistency of the SCJGNNs is observed by using the process of correlation, histogram curves, regression, and function fitness.

Keywords: scale conjugate gradient; malaria disease; neural networks; mathematical model; numerical solutions

Mathematics Subject Classification: 68T07, 92B20, 65L06

1. Introduction

There are many life-threatening diseases, out of which Malaria is one of them that is produced through the parasite known as Plasmodium that transmits to humans with the infected anopheles mosquito bite [1–3]. People with malaria are infected by the Protozoan parasite, which grows within the cells of red blood and spreads the illness. There are four Plasmodia species that can become the reason of infection, known as oval, falciparum, malaria, and vivax, while the two other most widespread Plasmodium species are falciparum and vivax [4]. Malaria affects lots of people each year, mainly in South Asia, Africa, and South America. It becomes the major reason of death and illness in various developing regions, specifically young children, and pregnant women. The main symptoms of malaria are fever, muscle pain, and headache. Malaria can progress promptly, possibly severe anemia, lung problems, and even cause death. There are various effective tactics that proposed the World Health Organization (WHO) to treat and prevent this dangerous disease. Some of them are indoor spraying, pesticide-treated bed nets, and some antimalarial medications. The vector control systems can be applied to lessen the poisoned mosquito population. In general, malaria is a substantial global health task, which needs a comprehensive approach for its cure by using the strategies of vector control and early identification for its treatment.

Malaria is a dynamic and complicated disease, which is considered difficult to present its model mathematically. The malaria parasite's life cycle is complex due to numerous phases of development both in mosquito vector and human host. These points are prompted by numerous features, e.g., mosquito actions, host immunity, and environmental environments that is used to make difficult the disease dynamics to predict and understand. The intricacy of the virus's spread dynamics is one of the main problems with malaria modelling. Malaria spread is influenced by numerous interrelated influences, e.g., the mosquito vector density, the host immunity degree, and the accessibility of efficient mediations. The relations between these aspects indicate the nonlinearity and hard to capture using the mathematical systems [5]. However, the mathematical malaria disease model based on the pesticides and medication (MDMPM) is presented, which is categorized in four human (susceptible, exposed, infected, recovered) and two vector (susceptible, infected) classes. The pathogen infects the population of host then the individuals are categorized into groups based on the parasites number and virus types. Kermack–McKendrick [6] proposed the mathematical SEIRSI model based on the population of human/vector groups. The nonlinear dynamics of the SEIRSI model is presented as [7]:

$$\begin{aligned}
S_h^{'}(x) &= \alpha_h + \beta_1 R_h(x) - \gamma_1 \psi I_h(x) S_h(x) - \gamma_2 \xi I_m(x) S_h(x) - (\delta_1 + \eta_h) S_h(x),\\
E_h^{'}(x) &= \gamma_2 \xi I_m(x) S_h(x) + \gamma_1 \psi I_h(x) S_h(x) - (\beta_2 + \delta_2 + \eta_h) E_h(x),\\
I_h^{'}(x) &= \beta_2 E_h(x) - (\varepsilon + p\upsilon + \eta_h) I_h(x),\\
R_h^{'}(x) &= \delta_1 S_h(x) + \upsilon p I_h(x) + \delta_2 E_h(x) - (\beta_1 + \eta_h) R_h(x),\\
S_m^{'}(x) &= \alpha_m - (\sigma + \eta_m) S_m(x) - \gamma_3 e S_m(x) I_h(x),\\
I_m^{'}(x) &= \gamma_3 e I_h(x) S_m(x) - (\sigma + \eta_m) I_m(x).
\end{aligned} \tag{1}$$

The compartmental illustration of the *SEIRSI* model based on the MDMPM is shown in Figure 1, while the description of each parameter is given in Table 1.

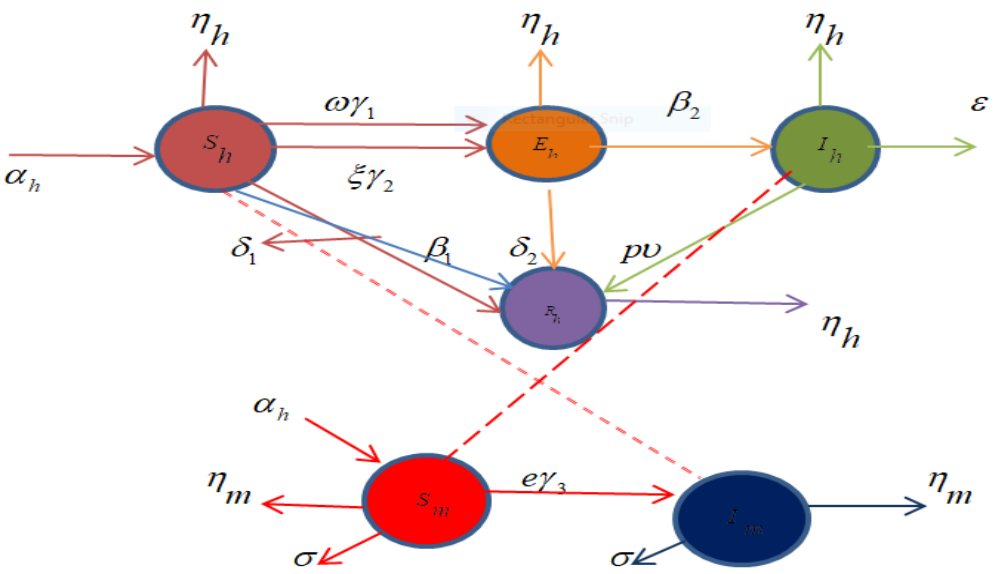

Figure 1. Graphical representations of the MDMPM.

Table 1. Parameter details of the MDMPM.

Parameters	**Details**
β_1	Susceptible form of recovered individuals
α_m	Newborn mosquitoes transfer rate into S_m
α_h	Newborns ratio to enter in S_h
γ_1	Transfer ratio of illness from one affected to susceptible people
ψ	Transfusions rate of average blood with stable time in I_h and S_h
β_2	Exposed to infected infection rate in people
ξ	Infected mosquito susceptible bites using fixed time
γ_3	Rate of Mosquitos infection
γ_2	Disease transfer through infected (mosquito) to susceptible (individual)
η_h	People natural rate of death
δ_2	Exposed recovered population
δ_1	Susceptible recovered population
p	Rate of humans heal
ε	Infected human death due to disease
η_m	Mosquitos' natural death
υ	Anti-malarial prescriptions
e	Bites S_m using the infected humans
σ	Expires sections using spraying for S_m and I_m
x	Time

There are various deterministic and conventional numerical schemes that have been presented to solve the biological models, including the wavelet Bernstein scheme that has been presented to solve the epidemic SIR fractional kind of infectious disease model [8], Laplace method is applied for the fractional epidemic system of born vector disease [9], q-homotopy transform technique is proposed to solve the fractional Schistosomiasis disease model [10,11], a theoretic investigation is presented based on the impacts of vector-virus transmission mechanism [12], a collocation technique with shifted Chebyshev polynomials is applied to solve the fractional order diseased model of Rubella ailment [13], an analytical computational approach is provided for the inflammatory atherosclerosis disease system [14], the differential stomach and coronavirus models have been discussed numerically by applying the Adam method [15,16] and the design of a numerical method is presented for the maturing communication in population and epidemic models [17]. Some more deterministic procedures that have been applied to solve different dynamical models are presented in [18–22].

All mentioned schemes have their individual strength, and demerits, however the stochastic solvers have never been tested before for the nonlinear dynamics of the MDMPM. The current study is related to the numerical solutions of the MDMPM through the stochastic procedures using the scale conjugate gradient neural networks (SCJGNNs). In recent years, the stochastic computing paradigms have been proposed in various applications, e.g., eye surgery differential systems [23,24], food chain systems [25,26], smoking dynamical systems [27], models arising in biological applications, [28,29], thermal explosion singular systems [30,31], and many more [32–43]. Based on these noteworthy applications of neuro-computing paradigm, the authors are motivated to present the numerical solutions of the malaria disease model of pesticides and medication (MDMPM) with stochastic framework of scale conjugate gradient neural networks (SCJGNNs). The purpose of this work is to provide a stochastic framework based on the SCJGNNs for solving the mathematical model representing MDMPM dynamics.

The contributions, insights and innovative aspects of the current scheme is portrayed in terms of salient features as follows:

- A novel design of the stochastic framework via SCJGNNs is introduced/presented to get the numerical results/outcomes of the nonlinear dynamics of governing mathematical model of MDMPM.
- The capability and knacks of Runge-Kutta solver is exploited/developed to formulate the target datasets for different scenario of MDMPM system that are used for the testing, and training procedure of the networks via SCJGNNs.
- The exactness of the stochastic SCJGNNs is attained/verified/validated through the overlapping of the results with standard counterparts having very small magnitude of absolute error (AE).
- The reliable matching of the numerical results, a strong arrangement using the benchmark outputs along with consistent statistical performance indices further prove the importance/significance/role of the SCJGNNs to solve the variant of MDMPM models.

The remaining paper is presented as: Proposed SCJGNNs design is shown in Section 2, Sect 3 presents the numerical results, and the conclusions are discussed in the final section.

2. Proposed SCJGNNs scheme

The current section is used to design the computing SCJGNNs structure to solve the MDMPM in

two steps, including the detail of designed SCJGNNs performances along with its execution. The designed SCJGNNs is presented in Figure 2. In the 1st phase of Figure 2, the nonlinear mathematical system is illustrated, the stochastic methodology using the SCJGNNs is provided in the 2nd phase of Figure 2, while some results are presented in the last phase of Figure 2. The performances using the multi-layers network based on the structure of single neuron is illustrated in Figure 3.

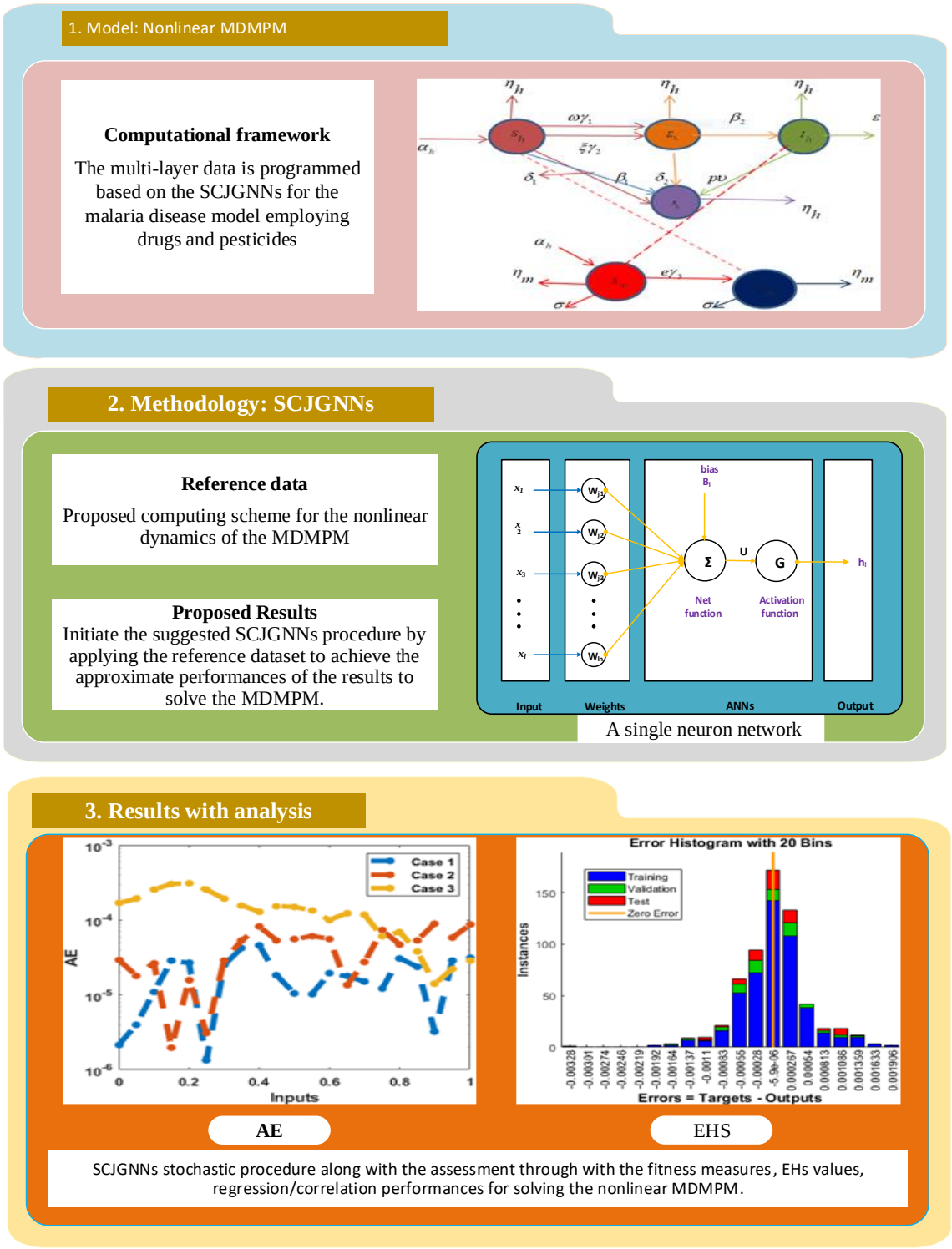

Figure 2. Illustration of proposed SCJGNNs performances to solve the MDMPM.

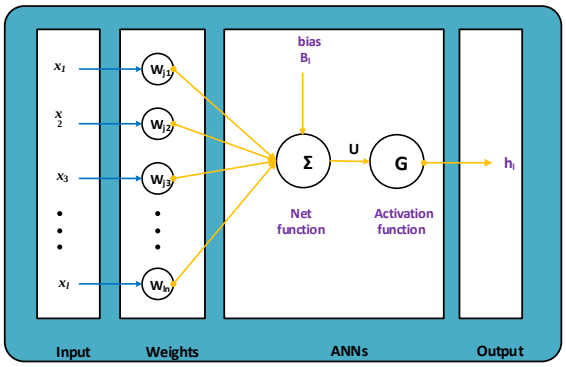

Figure 3. Single layer neural network.

The computing SCJGNNs approach for solving the MDMPM is executed using the command 'nftool' in software 'MATLAB', *n*-folded cross authentication, layers (output/hidden/input) structure, epochs are taken maximum 1000, fifteen hidden neurons, transfer function log-sigmoid, stopping standards, SCJG algorithm, tolerances, and step size. The label statics and input/target training are achieved using the basic outputs by taking the statics of validation (12%), testing (10%), and training (78%) for the MDMPM.

The designed computing SCJGNNs for the solutions of the MDMPM is performed by using 15 neurons, which have been validated through the best values of underfitting and overfitting based on the authorization and training at epochs 100, 86 and 69. For small neurons, the premature convergence (under fitting) problem is faced, while similar precision by using higher intricacy (overfitting issue) is noticed by taking higher neurons. The trials have been taken for the validation (12%), testing (10%), and training (78%) to solve the MDMPM. By taking a smaller data training, like 40% to 60%, the MSE values for testing 30% to 40% increase and generally poor presentations have been observed. On the other hand, if the training statics is almost designated > 90% and 5% for both testing and certification, the procedure's correctness improves marginally by choosing the label static, which presents the bias and targets input, but stochastic procedure's strength is not severely established for unbiased statics exclusive based targets information. The proposed values are performed on the input [0, 1] by applying the stochastic SCJGNNs procedure for the numerical performances of the MDMPM. The neuron structure using the input, output and hidden layers is shown in Figure 4.

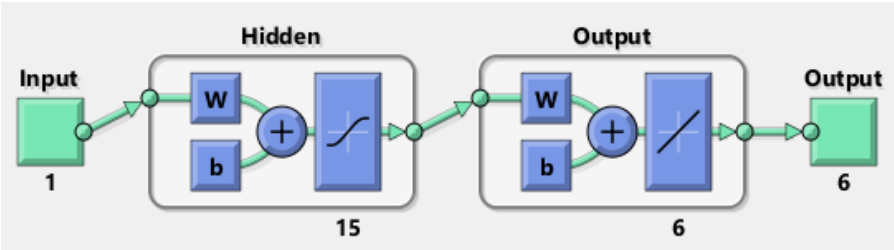

Figure 4. Different layers structure for the MDMPM.

3. Results and analysis

The numerical solution for three different cases of the MDMPM by applying the computing

procedures based on the SCJGNNs is presented in this section.

Case 1: Consider the values $\psi = 0.038$, $\alpha_h = 0.027$, $\gamma_1 = 0.020$, $\xi = 0.13$, $\beta_1 = \frac{1}{730}$, $\gamma_2 = 0.010$, $\delta_1 = 0.001$, $\eta_h = 0.0004$, $\delta_2 = 0.001$, $p = 0.611$, $\beta_2 = 0.001$, $\varepsilon = 0.05$, $\upsilon = 0.01$, $e = 0.022$, $\alpha_m = 0.13$, $\gamma_3 = 0.072$, $S_h(0) = 0.01$, $E_h(0) = 0.02$, $I_h(0) = 0.03$, $R_h(0) = 0.04$, $S_m(0) = 0.05$, and $I_m(0) = 0.06$ in system (1), which is shown as:

$$\begin{cases} S_h'(x) = 0.027 + 0.0014R_h(x) - (0.00076I_h(x) + 0.0014 + 0.0013I_m(x))S_h(x), & (S_h)_0 = 0.01, \\ E_h'(x) = (0.00076I_h(x) + 0.0013I_m(x))S_h(x) - 0.0024E_h(x), & (E_h)_0 = 0.02, \\ I_h'(x) = -0.00752I_h(x) + 0.001E_h(x), & (I_h)_0 = 0.03, \\ R_h'(x) = 0.00611I_h(x) - 0.00177R_h(x) + 0.001E_h(x) + 0.001S_h(x), & (R_h)_0 = 0.04, \\ S_m'(x) = 0.13 - 0.05S_m(x) - 0.001584I_h(x)S_m(x), & (S_m)_0 = 0.05, \\ I_m'(x) = 0.001584S_m(x)I_h(x) - 0.05I_m(x), & (I_m)_0 = 0.06. \end{cases} \tag{2}$$

Case 2: Consider the parameter values $\psi = 0.038$, $\alpha_h = 0.027$, $\gamma_1 = 0.020$, $\xi = 0.13$, $\beta_1 = \frac{1}{730}$, $\gamma_2 = 0.010$, $\delta_1 = 0.001$, $\eta_h = 0.0004$, $\delta_2 = 0.001$, $p = 0.611$, $\beta_2 = 0.001$, $\varepsilon = 0.05$, $\upsilon = 0.01$, $e = 0.022$, $\alpha_m = 0.13$, $\gamma_3 = 0.072$, $S_h(0) = 0.02$, $E_h(0) = 0.03$, $I_h(0) = 0.04$, $R_h(0) = 0.05$, $S_m(0) = 0.06$, and $I_m(0) = 0.07$ in system (1) that is given as:

$$\begin{cases} S_h'(x) = 0.027 + 0.0014R_h(x) - (0.00076I_h(x) + 0.0014 + 0.0013I_m(x))S_h(x), & (S_h)_0 = 0.02, \\ E_h'(x) = (0.00076I_h(x) + 0.0013I_m(x))S_h(x) - 0.0024E_h(x), & (E_h)_0 = 0.03, \\ I_h'(x) = -0.00752I_h(x) + 0.001E_h(x), & (I_h)_0 = 0.04, \\ R_h'(x) = 0.00611I_h(x) - 0.00177R_h(x) + 0.001E_h(x) + 0.001S_h(x), & (R_h)_0 = 0.05, \\ S_m'(x) = 0.13 - 0.05S_m(x) - 0.001584I_h(x)S_m(x), & (S_m)_0 = 0.06, \\ I_m'(x) = 0.001584S_m(x)I_h(x) - 0.05I_m(x), & (I_m)_0 = 0.07. \end{cases} \tag{3}$$

Case 3: Consider $\psi = 0.038$, $\alpha_h = 0.027$, $\gamma_1 = 0.020$, $\xi = 0.13$, $\beta_1 = \frac{1}{730}$, $\gamma_2 = 0.010$, $\delta_1 = 0.001$, $\eta_h = 0.0004$, $\delta_2 = 0.001$, $p = 0.611$, $\beta_2 = 0.001$, $\varepsilon = 0.05$, $\upsilon = 0.01$, $e = 0.022$, $\alpha_m = 0.13$, $\gamma_3 = 0.072$, $S_h(0) = 0.03$, $E_h(0) = 0.04$, $I_h(0) = 0.05$, $R_h(0) = 0.06$, $S_m(0) = 0.07$, and $I_m(0) = 0.08$ in system (1), given as:

$$\begin{cases} S_h'(x) = 0.027 + 0.0014R_h(x) - (0.00076I_h(x) + 0.0014 + 0.0013I_m(x))S_h(x), & (S_h)_0 = 0.03, \\ E_h'(x) = (0.00076I_h(x) + 0.0013I_m(x))S_h(x) - 0.0024E_h(x), & (E_h)_0 = 0.04, \\ I_h'(x) = -0.00752I_h(x) + 0.001E_h(x), & (I_h)_0 = 0.05, \\ R_h'(x) = 0.00611I_h(x) - 0.00177R_h(x) + 0.001E_h(x) + 0.001S_h(x), & (R_h)_0 = 0.06, \\ S_m'(x) = 0.13 - 0.05S_m(x) - 0.001584I_h(x)S_m(x), & (S_m)_0 = 0.07, \\ I_m'(x) = 0.001584S_m(x)I_h(x) - 0.05I_m(x), & (I_m)_0 = 0.08. \end{cases} \tag{4}$$

The plots of the estimated results based on the numerical SCJGNNs procedure for solving the MDMPM are shown in Figures 5 to 9. Figure 5 presents the best validation measures and state transitions for the nonlinear dynamics of the MDMPM through the stochastic computing SCJGNNs

scheme. The values of the mean square error (MSE) and the state of transition values are depicted in Figure 5. The computed performances of MSE using the best curves plots, certification, and training are provided in Figure 5(a–c) and the SoT measures are portrayed in Figure 5(d–f). The best solution performances of the MDMPM are shown at epochs 100, 86 and 69, which are found around 1.69774 $\times 10^{-07}$, 1.4324×10^{-07} and 3.5876×10^{-07}. It indicates that convergence through the MSE is observed based on dataset of training, testing and certification. It is also observed that by updating the epochs, the authentications, training, and testing graphs lead to steady-state position up to 10^{-07}. The gradient curves by applying the process of SCJGNNs to solve the MDMPM are calculated as 1.4161×10^{-06}, 8.1804×10^{-07} and 2.9486×10^{-06}. These graphic curves indicate the precision, exactness, and convergence by using the SCJGNNs procedure for the MDMPM. An error gradient presents the direction and magnitude that is calculated by the designed neural network for updating the weights in the proper amount/direction. In neural network fitting, the process of backpropagation is used to compute the loss function gradient. Mu is the used for the network's training for the momentum parameter, which includes the updated weight expressions to avoid the local minimum issues. It is observed that the network can stuck sometimes to the local minimum, which does not perform the convergence. In addition, Mu shows the control parameter based on that scheme that is used in the neural network's training.

Figure 6(a to c) presents the curves of fitting for the nonlinear MDMPM, which certifies the comparison of the results. Figure 6(d–f) signifies the error histogram (EH) values for the MDMPM by applying the computing SCJGNNs. The construction of EH is used to test the errors of the targeted and predicted values after the designed artificial neural network training. These errors present that how predicted measures contrast from the targeted values. These values based on the EH are obtained as 1.95×10^{-05}, 8.64×10^{-05} and -5.90×10^{-06} for respective dynamics of the MDMPM. Figures 7 to 9 present the correlation values for the MDMPM using the SCJGNNs. These measures based on the determination coefficient R^2 are found as 1 for each case of the MDMPM. The graphs of substantiation, testing, and training verify the correctness of the MDMPM using the numerical stochastic SCJGNNs procedure. The values of MSE convergence using the train, epochs, certification, backpropagation, test, and intricacy are tabulated in Table 2. The complexity measures using the SCJGNNs for the MDMPM are performed to authenticate the intricacy based on the network's training, i.e., epoch execution.

Table 2. MSE performances for solving the MDMPM.

Case	MSE for instances of sampling			Gradient	Performance	Epoch	Time
	Test	validation	Train				
I	2.745×10^{-07}	1.697×10^{-07}	2.366×10^{-07}	1.42×10^{-06}	2.26×10^{-07}	100	2 Sec
II	1.795×10^{-07}	1.432×10^{-07}	1.920×10^{-07}	8.18×10^{-07}	1.91×10^{-07}	86	2 Sec
III	5.112×10^{-07}	3.038×10^{-07}	3.678×10^{-07}	2.94×10^{-06}	2.09×10^{-07}	69	2 Sec

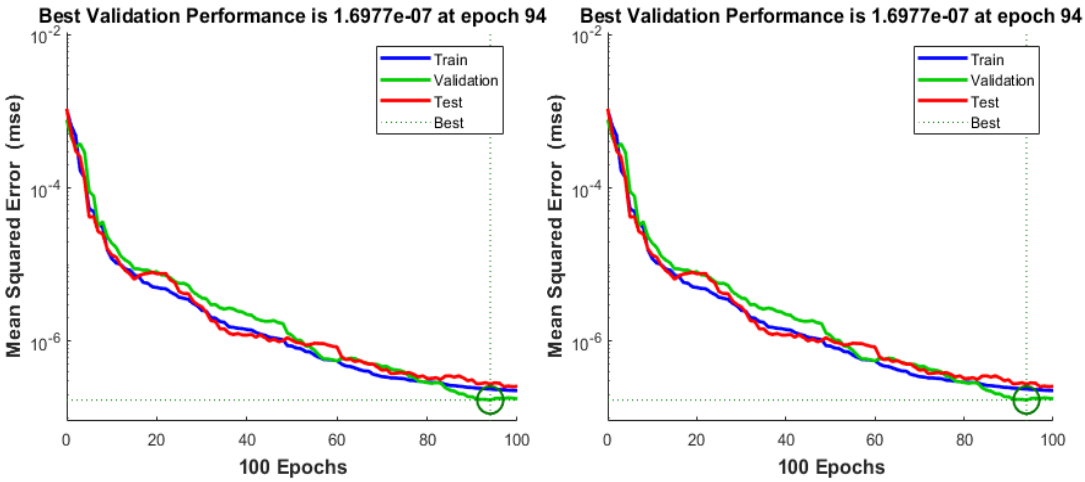

(a) Best validation performances for case 1 (b) Best validation performances for case 2.

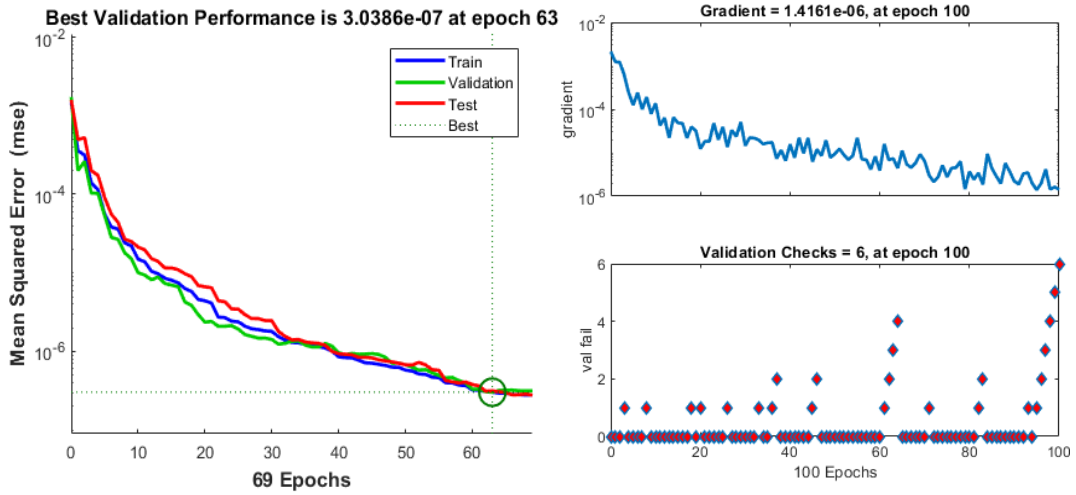

(c) Best validation performances for case 3. (d) State transition values for case 1.

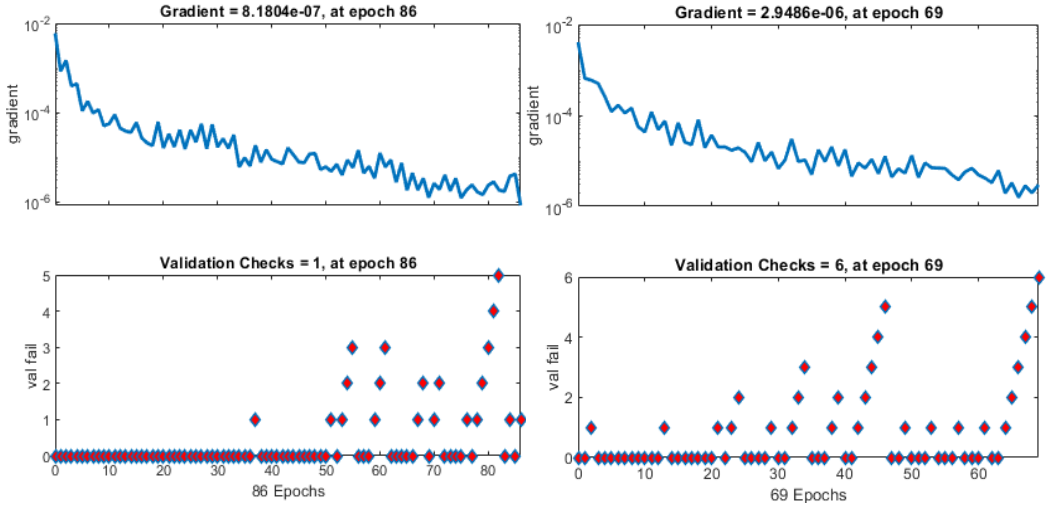

(e) State transition values for case 2. (f) State transition values for case 3.

Figure 5. Best validation measures and state transitions for the nonlinear dynamics of the MDMPM by applying the stochastic computing SCJGNNs procedure.

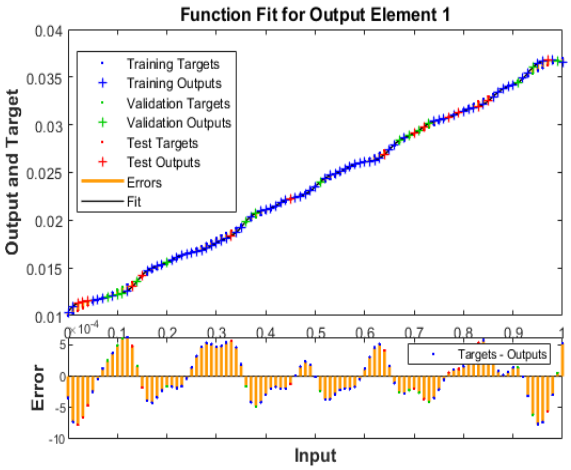

(a) Function fitness for case 1.

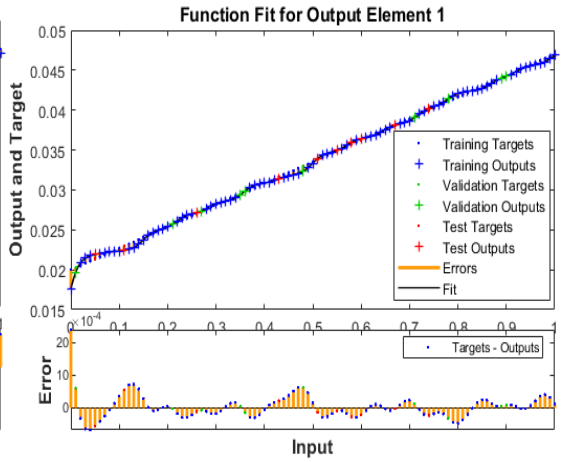

(b) Function fitness for case 2.

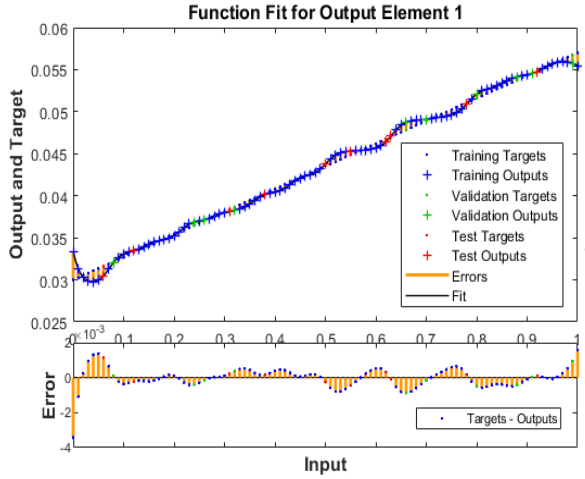

(c) Function fitness for case 3.

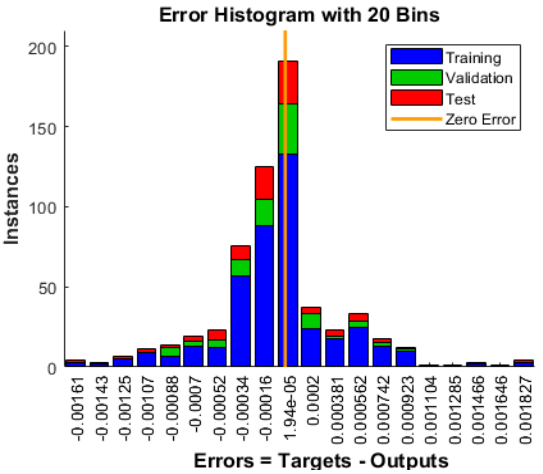

(d) Error histogram measures for case 1.

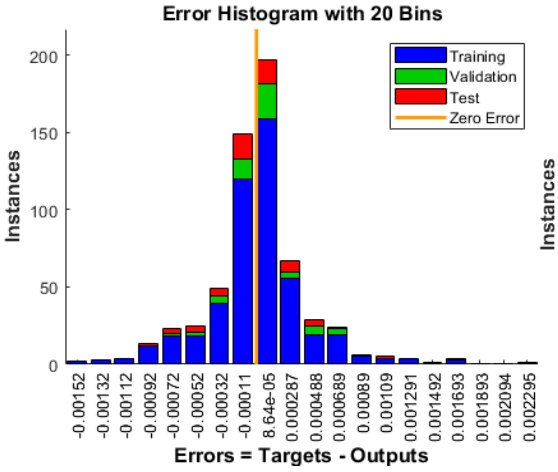

(e) Error histogram measures for case 2.

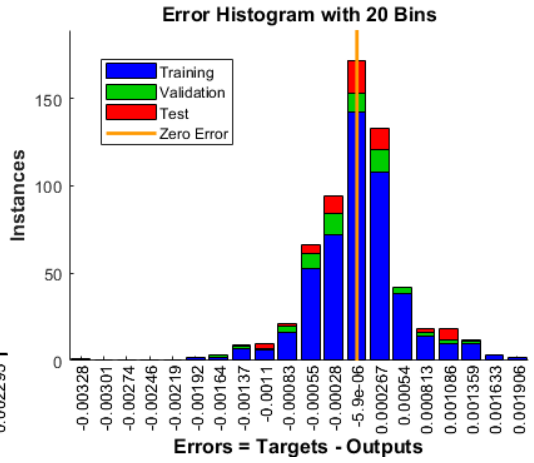

(f) Error histogram measures for case 3.

Figure 6. Function fitness values and error histogram performances to solve the MDMPM by applying the SCJGNNs.

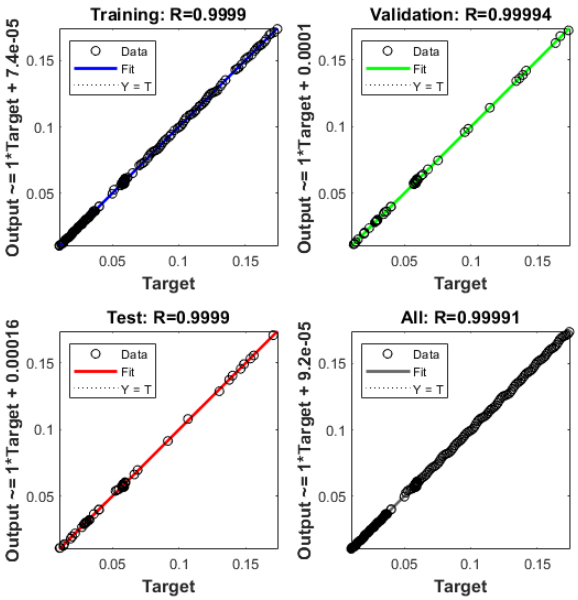

Figure 7. Values of regression for the MDMPM (1).

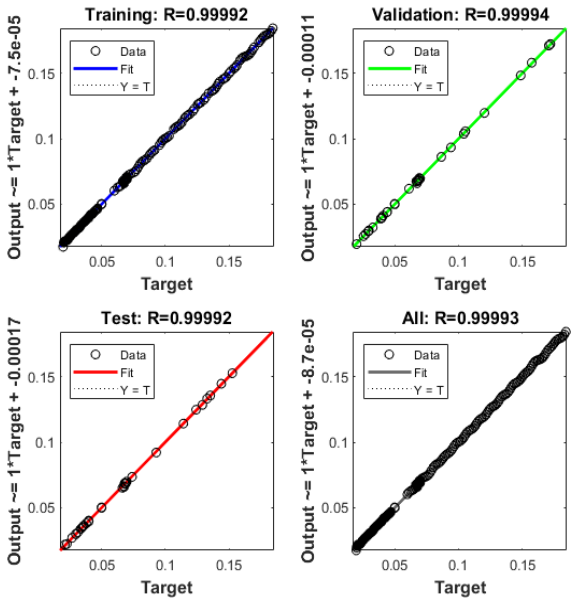

Figure 8. Values of regression for the MDMPM (2).

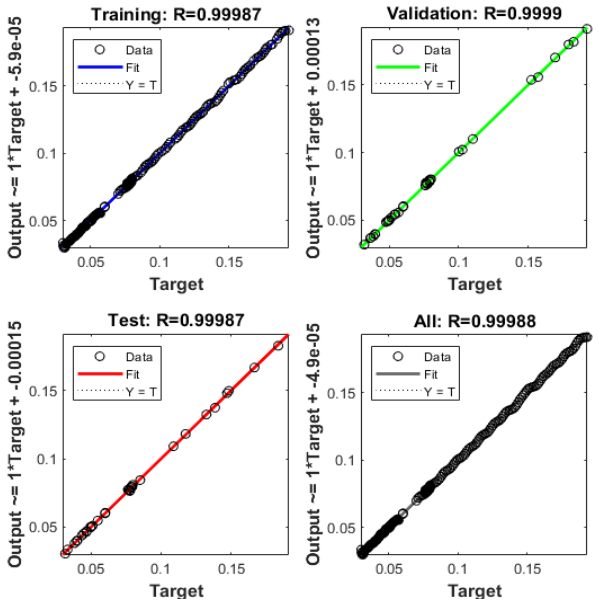

Figure 9. Values of regression for the MDMPM (3).

Figures 10 and 11 present the comparison graphs and AE using the obtained and source statics for the MDMPM. It is demonstrated that the source and calculated outcomes of the MDMPM precisely coincided. Figure 10 represents the AE graphs for each category of the MDMPM. For the first class, the AE lies as 10^{-03} to 10^{-05} for case I and III and 10^{-02} to 10^{-04} for case II. These values for the 2nd category of the MDMPM are found around 10^{-05} to 10^{-06}, 10^{-04} to 10^{-06} and 10^{-03} to 10^{-05} for cases I, II and III. The AE measures for the 3rd dynamics of the MDMPM lie as 10^{-04} to 10^{-07}, 10^{-03} to 10^{-05} and 10^{-03} to 10^{-06} for respective cases. These values for the 4th class of the MDMPM are calculated as 10^{-03} to 10^{-05} for case I and for case II and III, these AE are found as 10^{-03} to 10^{-04}.

The AE values for the 5th and 6th dynamics are found as 10^{-03} to 10^{-05} for each case of the model. These reduceable AE measures provides the accuracy of the scheme for the MDMPM.

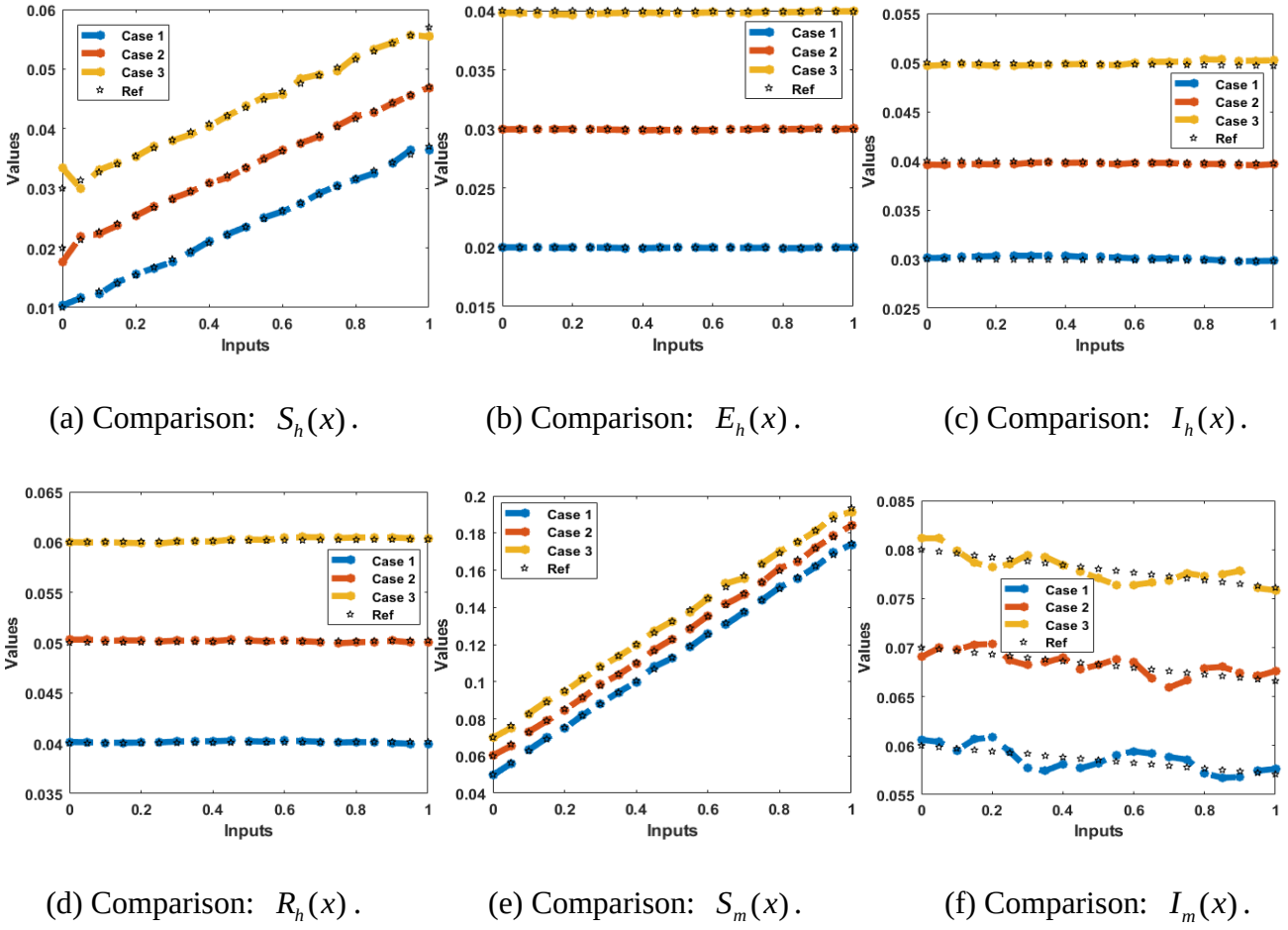

(a) Comparison: $S_h(x)$. (b) Comparison: $E_h(x)$. (c) Comparison: $I_h(x)$.

(d) Comparison: $R_h(x)$. (e) Comparison: $S_m(x)$. (f) Comparison: $I_m(x)$.

Figure 10. Achieved and reference results of the nonlinear MDMPM.

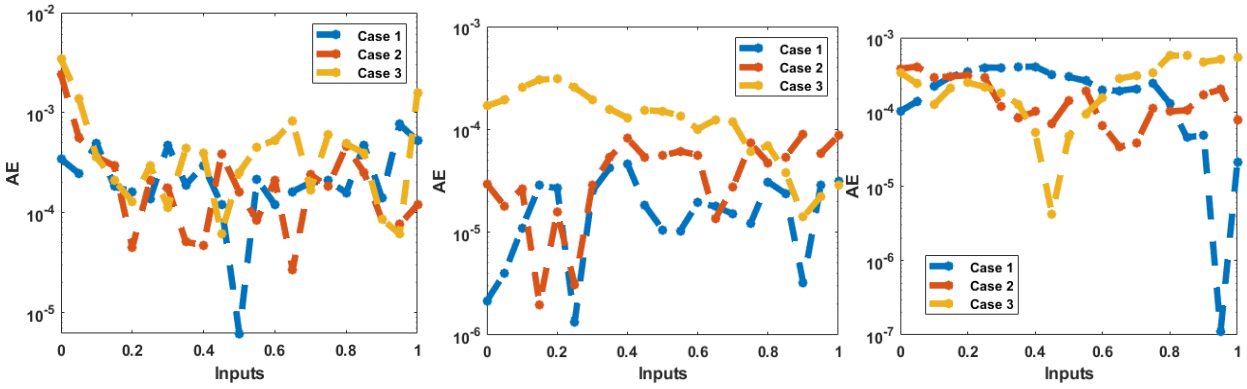

(a) AE of class 1 (b) AE of class 2 (c) AE of class 3

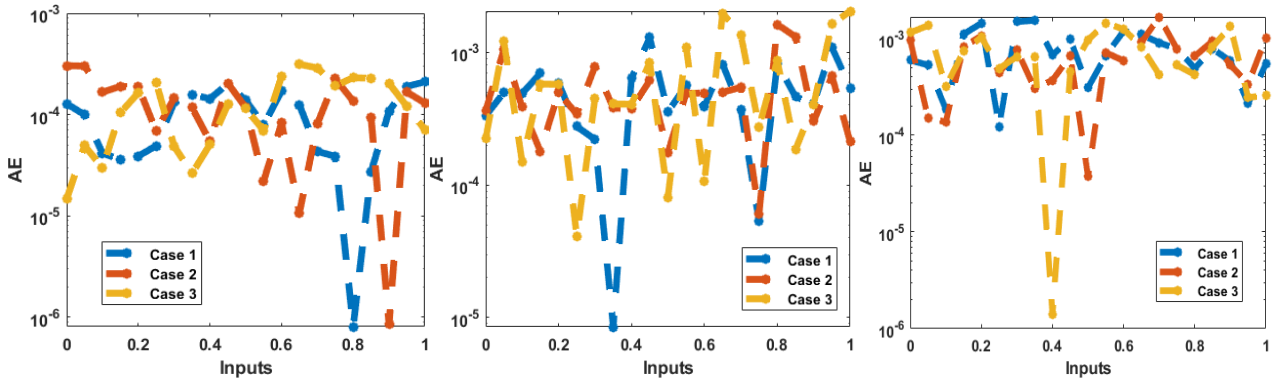

(d) AE of class 4 (e) AE of class 5 (f) AE of class 6

Figure 11. The values of the AE for the nonlinear MDMPM.

5. Conclusions

The stochastic numerical performances of the malaria disease using the pesticides and medication have been presented in this study. The populations-based host and vector are divided in the mathematical classification of the malaria using the pesticides and medication. Some conclusions of this work are reported as:

- The stochastic scale conjugate gradient neural network framework has been designed successfully for the numerical malaria disease model.
- The neural network procedure is presented by using fifteen neurons along with the log-sigmoid transfer function in the hidden layers to solve the model.
- The supervised neural networks process using the data as for validation 12%, testing 10%, and training 78% is presented for the numerical solutions of the system.
- The accuracy of the proposed stochastic scheme is examined through the overlapping of the achieved obtained and Runge-Kutta source solutions.
- The negligible performances of AE indicate the exactness of the computing stochastic approach.
- The consistency and trustworthiness of the designed procedure are assessed through the correlation, histogram curves, regression, and functional fitness process to solve the MDMPM.
- The perks/advantages of the proposed stochastic SCJGNNs procedure includes simplicity of the concept and understanding, straightforwardness in implementations and execution, provision of outcome on continuous domain, expandability and applicability.

The limitation/disadvantage of the stochastic SCJGNNs paradigm is the issue of trapping in local minima for scale conjugate gradient methodology while training of the weights of the networks, however, the said limitation is rectified by exploited heuristic global search methodologies in future by the interested readers. Additionally, in future, the designed SCJGNNs procedure can be explored/implemented for different applications of the nonlinear mathematical models arising in the field of computational fluid mechanics.

Conflict of interest

The authors declare that they have no conflict of interest

Authors' contributions

Manal Alqhtani: Conceptualization, methodology, validation, Writing-original draft preparation, writing-review; J.F. Gómez-Aguilar: Conceptualization, methodology, validation, investigation, Writing-original draft preparation, writing-review; Khaled M. Saad: Conceptualization, methodology, validation, writing-review and editing; Zulqurnain Sabir: Validation, investigation, Writing-original draft preparation, writing-review; Eduardo Pérez-Careta: Validation, formal analysis, investigation. All authors have read and agreed to the published version of the manuscript.

Acknowledgement

The authors are thankful to the Deanship of Scientific Research at Najran University for funding this work under the General Research Funding program grant code (NU/RG/SERC/12/22).

Use of AI tools declaration

The authors declare they have not used Artificial Intelligence (AI) tools in the creation of this article.

References

1. L. Cai, M. Martcheva, X. Z. Li, Epidemic models with age of infection, indirect transmission and incomplete treatment, *Discrete Cont. Dyn-B,* **18** (2013), 2239. https://doi.org/10.3934/dcdsb.2013.18.2239
2. K. W. Blayneh, J. Mohammed-Awel, Insecticide-resistant mosquitoes and malaria control, *Math. Biosci.,* **1** (2014), 252, 14–26. https://doi.org/10.1016/j.mbs.2014.03.007
3. B. A. Johnson, M. G. Kalra, Prevention of malaria in travelers, *Am. Fam. Physician,* **85** (2012)**,** 973–977.
4. A. Prabowo, Malaria: Mencegah dan Mengatasi, Niaga Swadaya, 2004.
5. B. Breedlove, Public health posters take aim against bloodthirsty ann, *Emerg. Infect. Dis.,* **27** (2021), 676. https://doi.org/10.3201/eid2702.AC2702
6. L. Basnarkov, I. Tomovski, T. Sandev, L. Kocarev, Non-Markovian SIR epidemic spreading model of COVID-19, *Chaos, Soliton. Fract.,* **1** (2022), 112286. https://doi.org/10.1016/j.chaos.2022.112286
7. M. Sinan, H. Ahmad, Z. Ahmad, J. Baili, S. Murtaza, M. A. Aiyashi, et al., Fractional mathematical modeling of malaria disease with treatment & insecticides, *Results Phys.*, **34 (**2022), 105220. https://doi.org/10.1016/j.rinp.2022.105220
8. S. Kumar, A. Ahmadian, R. Kumar, D. Kumar, J. Singh, D. Baleanu, et al., An efficient numerical method for fractional SIR epidemic model of infectious disease by using Bernstein wavelets, *Mathematics*, **8** (2020), 558. https://doi.org/10.3390/math8040558

9. F. Haq, K. Shah, A. Khan, M. Shahzad, Numerical solution of fractional order epidemic model of a vector born disease by Laplace Adomian decomposition method, *Punjab Univ. J. Math.*, **49** (2020), 1–8.
10. P. Veeresha, E. Ilhan, D. G. Prakasha, H. M. Baskonus, W. Gao, A new numerical investigation of fractional order susceptible-infected-recovered epidemic model of childhood disease, *Alex. Eng. J.*, **61** (2022), 1747–1756. https://doi.org/10.1016/j.aej.2021.07.015
11. P. Veeresha, H. M. Baskonus, D. G. Prakasha, W. Gao, G. Yel, Regarding new numerical solution of fractional Schistosomiasis disease arising in biological phenomena, *Chaos, Soliton. Fract.*, **133** (2020), 109661. https://doi.org/10.1016/j.chaos.2020.109661
12. L.V. Madden, M. J. Jeger, F. Van den Bosch, A theoretical assessment of the effects of vector-virus transmission mechanism on plant virus disease epidemics, *Phytopathology*, **90** (2000), 576–594. https://doi.org/10.1094/PHYTO.2000.90.6.576
13. A. M. S. Mahdy, M. S. Mohamed, K. Lotfy, M. Alhazmi, A. A. El-Bary, M. H. Raddadi, Numerical solution and dynamical behaviors for solving fractional nonlinear Rubella ailment disease model, *Results Phys.*, **24** (2021), 104091. https://doi.org/10.1016/j.rinp.2021.104091
14. A. Hidalgo, L. Tello, E. F. Toro, Numerical and analytical study of an atherosclerosis inflammatory disease model, *J. Math. Biol.*, **68** (2014), 1785–1814. https://doi.org/10.1007/s00285-013-0688-0
15. Y. G. Sánchez, Z. Sabir, J. L. Guirao, Design of a nonlinear SITR fractal model based on the dynamics of a novel coronavirus (COVID-19), *Fractals*, **28** (2020), 2040026. https://doi.org/10.1142/S0218348X20400265
16. Y. Guerrero Sánchez, Z. Sabir, H. Günerhan, H. M. Baskonus, Analytical and approximate solutions of a novel nervous stomach mathematical model, *Discrete Dyn. Nat. Soc.*, **2020** (2020), 1–13. https://doi.org/10.1155/2020/5063271
17. K. Cooke, P. Van den Driessche, X. Zou, Interaction of maturation delay and nonlinear birth in population and epidemic models, *J. Math. Biol.*, **39** (1999), 332–352. https://doi.org/10.1007/s002850050194
18. T. Rhodes, Mathematical models as public troubles in COVID-19 infection control: Following the numbers, *Health Sociol. Rev.*, **29** (2020), 177–194. https://doi.org/10.1080/14461242.2020.1764376
19. D. Benvenuto, Application of the ARIMA model on the COVID-2019 epidemic dataset, *Data Brief*, **29** (2020), 105340. https://doi.org/10.1016/j.dib.2020.105340
20. A. Sivakumar, Review of mathematical models to predict the rate of spread and control of COVID-19 in India, Bull World Health Organ, 2020.
21. S. K. Mustafa, Brief review of the mathematical models for analyzing and forecasting transmission of COVID-19, 2020.
22. R. N. Thompson, Epidemiological models are important tools for guiding COVID-19 interventions, *BMC Med.*, **18** (2020), 1–4. https://doi.org/10.1186/s12916-020-01628-4
23. I. Ahmad, M. A. Z. Raja, H. Ramos, M. Bilal, M. Shoaib, Integrated neuro-evolution-based computing solver for dynamics of nonlinear corneal shape model numerically, *Neural Comput. Appl.*, **33** (2021), 5753–5769. https://doi.org/10.1007/s00521-020-05355-y
24. B. Wang, J. F. Gómez-Aguilar, Z. Sabir, M. A. Z. Raja, W. F. Xia, H. Jahanshahi, et al., Numerical computing to solve the nonlinear corneal system of eye surgery using the capability of Morlet wavelet artificial neural networks, *Fractals*, **1** (2022), 2240147. https://doi.org/10.1142/S0218348X22401478

25. Z. Sabir, M. A. Z. Raja, S. R. Mahmoud, M. Balubaid, A. Algarni, A. H. Alghtani, et al., A novel design of morlet wavelet to solve the dynamics of nervous stomach nonlinear model, *Int. J. Comput. Int. Sys.,* **15** (2022), 1–4. https://doi.org/10.1007/s44196-021-00057-2
26. T. Mouktonglang, Z. Sabir, M. A. Z. Raja, S. Bhatti, T. Botmart, W. Weera, et al., Designing Meyer wavelet neural networks for the three-species food chain model, *AIMS Math.,* **8** (2023), 61–75. https://doi.org/10.3934/math.2023003
27. Z. Sabir, M. A. Z. Raja, A. S. Alnahdi, M. B. Jeelani, M. A. Abdelkawy, Numerical investigations of the nonlinear smoke model using the Gudermannian neural networks, *Math. Biosci. Eng.*, **19** (2022), 351–370. https://doi.org/10.3934/mbe.2022018
28. K. Mukdasai, Z. Sabir, M. A. Z. Raja, R. Sadat, M. R. Ali, P. Singkibud, A numerical simulation of the fractional order Leptospirosis model using the supervise neural network, *Alex. Eng. J.,* **61** (2022), 12431–12441. https://doi.org/10.1016/j.aej.2022.06.013
29. T. Botmart, Z. Sabir, M. A. Z. Raja, M. R. Ali, R. Sadat, A. A. Aly, et al., A hybrid swarming computing approach to solve the biological nonlinear Leptospirosis system, *Biomed. Signal Proces.,* **77** (2022), 103789. https://doi.org/10.1016/j.bspc.2022.103789
30. Z. Sabir, Neuron analysis through the swarming procedures for the singular two-point boundary value problems arising in the theory of thermal explosion, *Eur. Phys. J. Plus*, **137** (2022), 638. https://doi.org/10.1140/epjp/s13360-022-02869-3
31. Z. Sabir, M. A. Manzar, M. A. Z. Raja, M. Sheraz, A. M. Wazwaz, Neuro-heuristics for nonlinear singular Thomas-Fermi systems, *Appl. Soft Comput.*, **65** (2018), 152–169. https://doi.org/10.1016/j.asoc.2018.01.009
32. H. Liu, T. Liu, Z. Zhang, A. K. Sangaiah, B. Yang, Y. Li, ARHPE: Asymmetric relation-aware representation learning for head pose estimation in industrial human–computer interaction, *IEEE T. Ind. Inform.*, **18** (2022), 7107–7117. https://doi.org/10.1109/TII.2022.3143605
33. H. Liu, T. Liu, Y. Chen, Z. Zhang, Y. F. Li, EHPE: Skeleton cues-based gaussian coordinate encoding for efficient human pose estimation, *IEEE T. Multimedia*, **1** (2022), 1–16. https://doi.org/10.1109/TMM.2022.3197364
34. H. Liu, S. Fang, Z. Zhang, D. Li, K. Lin, J. Wang, MFDNet: Collaborative poses perception and matrix Fisher distribution for head pose estimation, *IEEE T. Multimedia*, **24** (2021), 2449–2460. https://doi.org/10.1109/TMM.2021.3081873
35. H. Ilyas, I. Ahmad, M. A. Z. Raja, M. Shoaib, A novel design of Gaussian WaveNets for rotational hybrid nanofluidic flow over a stretching sheet involving thermal radiation, *Int. Commun. Heat Mass,* **123** (2021), 105196. https://doi.org/10.1016/j.icheatmasstransfer.2021.105196
36. M. Dewasurendra, K. Vajravelu, On the method of inverse mapping for solutions of coupled systems of nonlinear differential equations arising in nanofluid flow, heat and mass transfer, *Appl. Math. Nonlin. Sci.,* **3** (2018), 1–14. https://doi.org/10.21042/AMNS.2018.1.00001
37. A. Yokuş, S. Gülbahar, Numerical solutions with linearization techniques of the fractional Harry Dym equation, *Appl. Math. Nonlin. Sci.,* **4** (2019), 35–42. https://doi.org/10.2478/AMNS.2019.1.00004
38. H. Rahaman, M. K. Hasan, A. Ali, M. S. Alam, Implicit methods for numerical solution of singular initial value problems, *Appl. Math. Nonlin. Sci.,* **6** (2021), 1–8. https://doi.org/10.2478/amns.2020.2.00001

39. A. H. Bukhari, M. A. Z. Raja, N. Rafiq, M. Shoaib, A. K. Kiani, C. M. Shu, Design of intelligent computing networks for nonlinear chaotic fractional Rossler system, *Chaos, Soliton. Fract.*, **157** (2022), 111985. https://doi.org/10.1016/j.chaos.2022.111985
40. X. Li, T. Li, S. Li, B. Tian, J. Ju, T. Liu, et al., Learning fusion feature representation for garbage image classification model in human-robot interaction, *Infrared Phys. Techn.*, **128** (2023), 104457. https://doi.org/10.1016/j.infrared.2022.104457
41. T. Liu, J. Wang, B. Yang, X. Wang, Facial expression recognition method with multi-label distribution learning for non-verbal behavior understanding in the classroom, *Infrared Phys. Techn.*, **112** (2021), 103594. https://doi.org/10.1016/j.infrared.2020.103594
42. T. Liu, J. Wang, B. Yang, X. Wang, NGDNet: Nonuniform Gaussian-label distribution learning for infrared head pose estimation and on-task behavior understanding in the classroom, *Neurocomputing*, **436** (2021), 210–220. https://doi.org/10.1016/j.neucom.2020.12.090
43. M. Shoaib, M. A. Z. Raja, M. T. Sabir, A. H. Bukhari, H. Alrabaiah, Z. Shah, et al., A stochastic numerical analysis based on hybrid NAR-RBFs networks nonlinear SITR model for novel COVID-19 dynamics, *Comput. Meth. Prog. Bio.*, **202** (2021), 105973. https://doi.org/10.1016/j.cmpb.2021.105973

AIMS Press